Near-infrared demonstration of computer-generated holograms implemented by using subwavelength gratings with space-variant orientation

Uriel Levy, Hyo-Chang Kim, Chia-Ho Tsai, and Yeshaiahu Fainman

Department of Electrical and Computer Engineering, University of California, San Diego, 9500 Gilman Drive, La Jolla, California 92093-0407

Received February 7, 2005

We provide an experimental demonstration of novel form-birefringent computer-generated holograms at wavelengths of 1.55 and 10.6 μm. These novel devices utilize a 2-D array of cells that can be fabricated with a single lithographic step. Each cell contains a subwavelength binary grating whose orientation controls the desired continuous phase profile within the cell. © 2005 Optical Society of America

OCIS codes: 260.5430, 050.1970.

Subwavelength-scale periodic inhomogeneous structures and birefringent computer-generated holograms (B-CGHs) have been engineered to artificially create unique anisotropic[1–3] and dispersive[4,5] characteristics. In recent years several authors have demonstrated phase modulation with B-CGH elements by fabricating subwavelength 1-D or 2-D gratings in each cell.[6–9] The desired phase modulation was achieved by controlling the duty cycle of the grating to modify the effective index within each cell based on the effective medium theory.[10] Nevertheless, precise control over the duty cycle during the fabrication process is difficult, practically limiting the number of phase levels that can be achieved, leading to quantization error. Moreover, effective-index modulation results in a significant variation in the local Fresnel reflection coefficient, effectively producing undesired amplitude modulation. This is particularly true for high-index semiconductor substrates used for devices in the near IR. For such substrates, reflection variations of the order of 10%–20% may occur. Recently, an approach for modulating the incident optical field by modifying the orientation of the subwavelength grating in a space-variant fashion[11,12] was presented. Similar to the previous approach, this implementation is also polarization sensitive, requiring the input polarization to be known in advance. Specifically, if the incident field is circularly polarized, controlling the orientation of the subwavelength grating provides pure phase modulation. Whereas a continuous rotation of subwavelength gratings has been successfully applied to demonstrate polarization transformers,[13,14] discrete 1-D and radially symmetric versions were used to implement array illuminators, polarization analyzers, and lenses with periodic phase function.[15–17] So far, these space-variant elements were demonstrated experimentally in only the far-IR regime (10.6 μm). In this Letter, we demonstrate for the first time (to the best of our knowledge) a 2-D form-birefringent computer-generated hologram (F-BCGH) having aperiodic phase distribution and operating at a wavelength of 1.55 μm. For comparison we also implement these concepts at the far-IR wavelength of 10.6 μm. Our device can be used for beam shaping, optical signal processing, polarization control, data storage, imaging, and more.

The operation of these F-BCGH elements is best understood with the effective-index approach[10] for gratings with a period much smaller than the wavelength of the optical field in the material. Due to differences in medium polarizability, the propagation of TE and TM (i.e., electric field perpendicular or parallel to the grating k vector, respectively) polarized fields will be similar to propagation in a negative uniaxial crystal, with a larger effective dielectric constant for the TE polarized light. With this approach, the F-BCGH is made of a 2-D array of cells (Fig. 1) where a subwavelength grating with a desired orientation and phase retardation is etched into each cell.

We consider a plane wave transmitted through the F-BCGH element located at $z=0$, with x and y being the transverse coordinates. Neglecting Fresnel reflections, the transmitted field is given by

$$E_T(x,y,z=0^+) = \bar{\bar{R}}(x,y)^{-1}\bar{\bar{G}}\bar{\bar{R}}(x,y)V_{in}, \qquad (1)$$

where

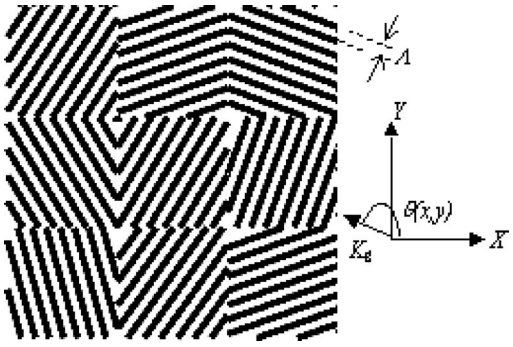

Fig. 1. Schematic diagram of the subwavelength-based array illuminator devices: A subwavelength grating with a period Λ is allocated into each cell. The orientation of the grating is given by $\theta(x,y)$.

0146-9592/05/162089-3/$15.00

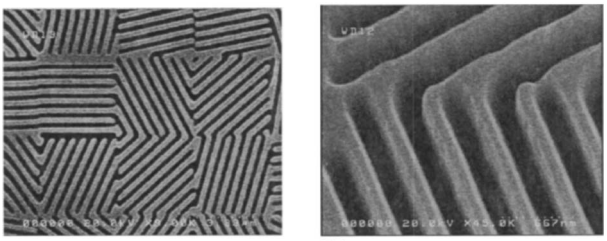

(a) (b)

Fig. 2. SEM photograph of the fabricated F-BCGH element for operation at a wavelength of 1.55 μm. (a) Typical top view; (b) enlarged slanted view.

$$\bar{\bar{R}}(x,y) = \begin{bmatrix} \cos[\theta(x,y)] & \sin[\theta(x,y)] \\ -\sin[\theta(x,y)] & \cos[\theta(x,y)] \end{bmatrix},$$

$$\bar{\bar{G}}(x,y) = \begin{bmatrix} \exp[-i\phi(x,y)/2] & 0 \\ 0 & \exp[i\phi(x,y)/2] \end{bmatrix}$$

are the rotation and Jones matrices, respectively, and V_{in} is the incident field Jones vector. The matrix G describes the birefringence of the subwavelength grating in each cell. The phase retardation value $\phi(x,y)$ depends on the grating profile, depth, and refractive index of the substrate material. $\theta(x,y)$ is the orientation angle of the subwavelength grating in each cell (see Fig. 1). Notice that Eq. (1) is valid for thin-element approximation, which is justified as long as the cell size is large compared to the wavelength of the optical field. Because of practical considerations (ease of fabrication), we next assume a constant duty cycle and etch depth in each cell leading to space-invariant values of ϕ and G.

For right- and left-hand circularly polarized incident light with the corresponding Jones vectors $V_{inR} = [1,j]^T$ and $V_{inL} = [1,-j]^T$, we rewrite Eq. (1) as[13]

$$E_{TR}(x,y,z=0^+) = \cos(\phi/2)\begin{bmatrix} 1 \\ j \end{bmatrix} - j\sin(\phi/2)\exp[+j2\theta(x,y)]\begin{bmatrix} 1 \\ -j \end{bmatrix}, \quad (2a)$$

$$E_{TL}(x,y,z=0^+) = \cos(\phi/2)\begin{bmatrix} 1 \\ -j \end{bmatrix} - j\sin(\phi/2)\exp[-j2\theta(x,y)]\begin{bmatrix} 1 \\ j \end{bmatrix}, \quad (2b)$$

respectively.

For our application we eliminate the constant cosine term by designing the grating to produce π phase retardation ($\phi=\pi$). With such a design, the F-BCGH provides pure phase modulation where the obtained phase is twice the rotation angle. Therefore, the desired phase modulation can be achieved by simply varying the orientation of the periodic structure in each cell such that continuous phase modulation is achieved with a simple binary grating. This approach eliminates the need for complicated multiple-step fabrication procedures, significantly reducing the fabrication complexity and consequently the cost of the element. Note that slight fabrication imperfections (e.g., deviation in the grating depth or the duty cycle) will affect only the phase retardation ϕ and are not expected to drastically deteriorate the device performance since $\mathrm{d}\sin(\phi/2)/\mathrm{d}\phi \to 0$ as $\phi \to \pi$.

One of the most common applications of computer-generated holograms is far-field beam shaping. This task involves the conversion of an incident beam with a known amplitude and phase profile into a desired beam profile in the far field. Typically, the far-field intensity pattern is of major concern, whereas the far-field phase is of lesser importance and can be used as a degree of freedom for optimization of the device.

We next demonstrate the usefulness of our F-BCGH for the application of far-field beam shaping. We have already shown[17] that the far-field distributions generated by left and right circular polarization illumination are conjugated, meaning that the obtained intensity patterns are mirrored with respect to each other, and therefore the device operation is polarization sensitive. The device operation becomes polarization insensitive for the particular case where the desired far-field pattern is symmetric.[17]

Hereby, we describe the fabrication and characterization of a F-BCGH designed to generate a far-field image of "UCSD." We first optimize the phase profile to be generated by the F-BCGH by using an iterative Fourier-transform algorithm.[18] From Eq. (2), $\theta(x,y)$ is half of the optimized phase profile. To ensure that the desired structure is indeed equivalent to a uniaxial crystal, the subwavelength grating period needs to satisfy the inequality $\Lambda < \lambda/n$, where Λ is the period of the subwavelength grating, λ is the optical wavelength, and n is the refractive index of the substrate. With a GaAs substrate having a refractive index of 3.37 at $\lambda = 1.55$ μm, we used a period of $\Lambda = 400$ nm and a duty cycle of 50%. For these parameters, the desired etching depth for achieving π phase retardation was found (by using rigorous coupled-wave analysis[19]) to be 750 nm.

To fabricate the F-BCGH device, we employed electron-beam (E-beam) lithography followed by chemically assisted ion-beam etching (CAIBE). Writing the submicrometer patterns requires high magnification ($\sim$300 for our E-beam writing tool). With this magnification the field size of our E-beam writing tool is limited to $\sim$300 μm; thus we limit the array size to 90×90 cells, with a cell size of 3.25 μm. At first, the GaAs substrate was spin coated with a 300 nm thick E-beam resist (ZEP 520A). We then

Fig. 3. Far-field reconstruction for 1.55 μm. Speckle noise can be eliminated by replicating the phase function several times along the element plane.

(a) (b)

Fig. 4. Far-field reconstruction of an element operating at a wavelength of 10.6 μm. (a) Reconstruction achieved with right-hand circularly polarized light; (b) reconstruction achieved with linearly polarized light.

patterned the grating lines using our converted scanning electron microscope (SEM, JEOL JSM 6400) writing tool. We used CAIBE to transfer the pattern into a GaAs substrate that was coated with an antireflection layer on its backside to avoid surface reflection. Figure 2 shows top-view and slanted-view SEM images of the fabricated device.

To demonstrate the proposed approach for high-power CO_2 laser applications and to evaluate the effect of increasing the cell size, we fabricated an additional F-BCGH element for operation at the wavelength of 10.6 μm with the following parameters: 128×128 cells, cell size of 100 μm, $\Lambda = 2.5$ μm, duty cycle of 50%, and grating depth of 6 μm. The desired structure was generated on an E-beam mask and then transferred to the photoresist (BPRS100) by using photolithography. Finally, the patterns were etched into the GaAs substrate with CAIBE.

Characterization of the devices was performed with a circularly polarized beam derived from either a diode laser (New Focus) at 1.55 μm or a CO_2 laser (Synrad 48-1) at 10.6 μm. We used a quarter-wave plate to convert the linear polarization into circularly polarized input light. The F-BCGH element was illuminated with a converging beam such that the desired Fourier transform was obtained in its focal plane.

An element operating at 1.55 μm was placed 2 cm in front of the focal plane and the Fourier-transform image was captured with a CCD camera (Indigo NIR) (see Fig. 3). The letters "UCSD" can be clearly observed, although the quality is somewhat degraded due to both speckle noise and distortion resulting from the departure from the thin-element approximation as the cell size approaches the operating optical wavelength. The speckle pattern can be eliminated by replicating the phase function several times along the element aperture. The cell size can be increased by use of a commercial E-beam writer with a negligibly small stitching error, allowing a larger aperture for the F-BCGH element.

The element operating at the wavelength of 10.6 μm was placed 15 cm in front of the focal plane, and the reconstructed Fourier transform was imaged with a CCD camera (Indigo Omega). Figure 4(a) shows the far-field intensity pattern obtained with circularly polarized illumination. The quality of the reconstruction is now improved due to a larger cell size to wavelength ratio. Figure 4(b) shows the far-field intensity pattern obtained with a linearly polarized illumination field. As expected, a conjugate image appears since the linear polarization can be decomposed into equal strength left- and right-hand circular polarization components.

In conclusion, we have fabricated novel F-BCGHs and demonstrated experimentally a 2-D far-field beam-shaping application for operation at wavelengths of 1.55 and 10.6 μm. The devices were fabricated by etching a subwavelength grating with space-variant orientation into each cell of the 2-D array. The orientation of the grating was linearly proportional to the desired phase, allowing continuous phase modulation with a binary structure and significantly reducing the complexity of the fabrication process. These elements can be effectively used for various applications, such as beam shaping, optical signal processing, polarization control, data storage, and imaging.

This work was supported in part by the Air Force Office of Scientific Research, the National Science Foundation, the Defense Advanced Research Projects Agency, and the Space and Naval Warfare Systems Command. We thank Shayan Mookherjea for making his SEM imaging system available to us. U. Levy's e-mail address is ulevy@ece.ucsd.edu

References

1. I. Richter, P. C. Sun, F. Xu, and Y. Fainman, Appl. Opt. **34**, 2421 (1995).
2. F. Xu, R. Tyan, P. C. Sun, C. Cheng, A. Scherer, and Y. Fainman, Opt. Lett. **20**, 2457 (1995).
3. F. Xu, Y. Fainman, and J. E. Ford, Appl. Opt. **34**, 256 (1995).
4. G. Nordin and P. Deguzman, Opt. Express **5**, 163 (1999).
5. U. Levy and Y. Fainman, J. Opt. Soc. Am. A **21**, 881 (2004).
6. F. T. Chen and H. G. Craighead, Opt. Lett. **20**, 121 (1995).
7. P. Lalanne, S. Astilean, P. Chavel, E. Cambril, and H. Launois, Opt. Lett. **23**, 1081 (1998).
8. J. N. Mait, A. Scherer, O. Dial, D. W. Prather, and X. Gao, Opt. Lett. **25**, 381 (2000).
9. W. Yu, K. Takahara, T. Konishi, T. Yotsuya, and Y. Ichioka, Appl. Opt. **39**, 3531 (2000).
10. S. M. Rytov, Sov. Phys. JETP **2**, 466 (1956).
11. J. Tervo, V. Kettunen, M. Honkanen, and J. Turunen, J. Opt. Soc. Am. A **20**, 282 (2003).
12. Z. Bomzon, G. Biener, V. Kleiner, and E. Hasman, Opt. Lett. **27**, 1141 (2002).
13. Z. Bomzon, G. Biener, V. Kleiner, and E. Hasman, Opt. Lett. **27**, 285 (2002).
14. U. Levy, C. H. Tsai, L. Pang, and Y. Fainman, Opt. Lett. **29**, 1718 (2004).
15. G. Biener, A. Niv, V. Kleiner, and E. Hasman, J. Opt. Soc. Am. A **20**, 1940 (2003).
16. E. Hasman, V. Kleiner, G. Biener, and A. Niv, Appl. Phys. Lett. **82**, 328 (2003).
17. U. Levy, C. H. Tsai, H. C. Kim, and Y. Fainman, Opt. Express **12**, 5345 (2004).
18. O. Bryngdahl and F. Wyrowski, in *Progress in Optics*, E. Wolf, ed. (North-Holland, 1990), Vol. 28, Chap. 1.
19. M. G. Moharam and T. K. Gaylord, J. Opt. Soc. Am. **72**, 1385 (1982).